2003

Astrometry with The *Hubble Space Telescope*: A Parallax of the Central Star of the Planetary Nebula NGC 6853

G. Fritz Benedict

B. E. McArthur

See next page for additional authors

Citation/Publisher Attribution

Benedict, G. F., McArtur, B. E., Fredrick, L. W., Harrison, T. E., Skrutskie, M. F., Siesnick, C. L., Rhee, J.,...Bradley, A. J. (2003). Astrometry with The *Hubble Space Telescope*: A Parallax of the Central Star of the Planetary Nebula NGC 6853. *The Astronomical Journal, 126*(5), 2549-2556. doi: 10.1086/378603
Available at: https://doi.org/10.1086/378603

Authors
G. Fritz Benedict, B. E. McArthur, L. W. Fredrick, T. E. Harrison, M. F. Skrutskie, C. L. Slesnick, J. Rhee, R. J. Patterson, E. Nelan, W. H. Jefferys, W. van Altena, T. Montemayor, P. J. Shelus, O. G. Franz, L. H. Wasserman, P. D. Hemenway, R. L. Duncombe, D. Story, A. L. Whipple, and A. J. Bradley

The Astronomical Journal, 126:2549–2556, 2003 November

ASTROMETRY WITH THE *HUBBLE SPACE TELESCOPE*: A PARALLAX OF THE CENTRAL STAR OF THE PLANETARY NEBULA NGC 6853[1]

G. Fritz Benedict,[2] B. E. McArthur,[2] L. W. Fredrick,[3] T. E. Harrison,[4] M. F. Skrutskie,[3] C. L. Slesnick,[3] J. Rhee,[3] R. J. Patterson,[3] E. Nelan,[5] W. H. Jefferys,[6] W. van Altena,[7] T. Montemayor,[2] P. J. Shelus,[2] O. G. Franz,[8] L. H. Wasserman,[8] P. D. Hemenway,[9] R. L. Duncombe,[10] D. Story,[11] A. L. Whipple,[11] and A. J. Bradley[12]

Received 2003 May 12; accepted 2003 July 22

ABSTRACT

We present an absolute parallax and relative proper motion for the central star of the planetary nebula NGC 6853 (the Dumbbell). We obtain these with astrometric data from the Fine Guidance Sensor 3, a white-light interferometer on the *Hubble Space Telescope*. Spectral classifications and $VRIJHKT_2M$ and DDO51 photometry of the stars making up the astrometric reference frame provide spectrophotometric estimates of their absolute parallaxes. Introducing these into our model as observations with error, we find $\pi_{\rm abs} = 2.10 \pm 0.48$ mas for the DAO central star of NGC 6853. A weighted average with a previous ground-based USNO determination yields $\pi_{\rm abs} = 2.40 \pm 0.32$. We assume that the extinction suffered by the reference stars nearest (in angular separation and distance) to the central star is the same as for the central star. Correcting for color differences, we find $\langle A_V \rangle = 0.30 \pm 0.06$ for the central star, hence, an absolute magnitude $M_V = 5.48^{-0.16}_{+0.15}$. A recent determination of the central star effective temperature aided in estimating the central star radius, $R_* = 0.055 \pm 0.02\ R_\odot$, a star that may be descending to the white dwarf cooling track.

Key words: astrometry — planetary nebulae: individual (NGC 6853) — stars: distances — techniques: interferometric — white dwarfs

On-line material: color figure

1. INTRODUCTION

Planetary nebulae (PNs) are a visually spectacular and relatively short-lived step in the evolution from asymptotic giant branch (AGB) stars, to a final white dwarf stage. Iben & Renzini (1983) first showed that the ejection of most of the gaseous envelope in AGB stars occurs at the tip of the thermal pulse phase, in the form of a massive, low-velocity wind. As summarized by Stanghellini et al. (2002), the remnant central star (CS) ionizes the gaseous ejecta, while a fast, low mass-loss rate CS wind shapes the PN. PN morphology depends on a complicated combination of phenomena, some occurring within the nebular gas, which evolves in dynamic timescale, and others caused by the evolution of the stellar progenitors and of the CS. Morphology may also depend on the physical status of the interstellar environment of the PN progenitor. Intercomparison of PN can aid our understanding of the complicated astrophysics of this stage of stellar evolution, particularly if distances are known. Many indirect methods of PN distance determination exist (Ciardullo et al. 1999; Napiwotzki 2001). Agreement among these methods is seldom better than 20%. Direct parallax measurements of PN CSs rarely have precisions smaller than the measured parallax, a notable exception being Harris et al. (1997), who provide ~0.5 mas precision parallaxes for seven PNs CS nearer than 500 pc.

As the last object on the *Hubble Space Telescope* (*HST*) Astrometry Science Team list of astrophysically interesting stars, we have determined the absolute parallax of the CS of NGC 6853 (the Dumbbell, M27) using the Fine Guidance Sensor 3 (FGS 3). Napiwotzki (1999) classifies the CS as a white dwarf of type DAO. Our extensive investigation of the astrometric reference stars provides an independent estimation of the line-of-sight extinction to NGC 6853, a significant contributor to the uncertainty in the absolute magnitude, M_V, of its CS. We present the results of extensive spectrophotometry of the astrometric reference stars, required to correct our relative parallax to absolute; briefly discuss data acquisition and analysis; and derive an absolute parallax for the CS of NGC 6853. Finally, from a weighted average of our new result and that of Harris et al. (1997), we calculate an absolute magnitude for the CS and apply it to derive a stellar radius.

Bradley et al. (1991) and Nelan & Makidon (2002) provide an overview of the FGS 3 instrument and Benedict et al. (1999, 2002b) describe the fringe tracking (POS) mode astrometric capabilities of FGS 3, along with the data

[1] Based on observations made with the NASA/ESA *Hubble Space Telescope*, obtained at the Space Telescope Science Institute, which is operated by the Association of Universities for Research in Astronomy, Inc., under NASA contract NAS 5-26555.

[2] McDonald Observatory, University of Texas at Austin, Austin, TX 78712.
[3] Department of Astronomy, University of Virginia, P.O. Box 3818, Charlottesville, VA 22903.
[4] Department of Astronomy, New Mexico State University, Box 30001, MSC 4500, Las Cruces, NM 88003.
[5] Space Telescope Science Institute, 3700 San Martin Drive, Baltimore, MD 21218.
[6] Department of Astronomy, University of Texas at Austin, Austin, TX 78712.
[7] Department of Astronomy, Yale University, P.O. Box 208101, New Haven, CT 06520.
[8] Lowell Observatory, 1400 West Mars Hill Road, Flagstaff, AZ 86001.
[9] Department of Oceanography, University of Rhode Island, Kingston, RI 02881.
[10] Department of Aerospace Engineering, University of Texas at Austin, Austin, TX 78712.
[11] Aerospace Engineering Division, Jackson and Tull, Suite 200, 7375 Executive Place, Seabrook, MD 20706.
[12] Spacecraft System Engineering Services, P.O. Box 91, Annapolis Junction, MD 20706.

acquisition and reduction strategies used in the present study. We time-tag our data with a modified Julian Date, MJD = JD − 2,444,000.5, and abbreviate millisecond of arc, mas, throughout.

2. OBSERVATIONS AND DATA REDUCTION

Figure 1 shows the distribution of the seven reference stars and the CS relative to the brightest regions of the PN. This image, produced by compositing Johnson *B*, *V*, and *I* bandpass frames obtained with the McDonald Observatory 0.8 m telescope and Prime Focus Camera, reveals a particular difficulty with these data. The PN emission can contaminate the ancillary photometry and spectroscopy required to generate reference-star spectrophotometric parallaxes (§ 3). Eight sets of astrometric data were acquired with *HST*, spanning 2.59 yr, for a total of 140 measurements of the NGC 6853 CS and reference stars. Each data set required approximately 33 minutes of spacecraft time. The data were reduced and calibrated as detailed in Benedict et al. (2002b, 2002c) and McArthur et al. (2001). At each epoch, we measured reference stars and the target multiple times, this to correct for intraorbit drift of the type seen in the cross-filter calibration data shown in Figure 1 of Benedict et al. (2002b).

Table 1 lists the eight epochs of observation and highlights another particular difficulty with these data. We obtain observations at each of the two maximum parallax factors, hence the two distinct spacecraft roll values in Table 1. These are imposed by *HST* rolling to keep its solar panels fully illuminated throughout the year. This roll constraint generally imposes alternate orientations at each time of maximum positive or negative parallax factor over a typical 2.5 yr campaign, usually allowing a clean separation of parallax and proper-motion signatures. In this case, two guide star acquisition failures on two attempts at roll ~101° (along with a bookkeeping error in scheduling the makeup observation) left us with the less than satisfactory temporal segregation of orientations shown in Table 1. Only the first two epochs occur at maximum negative parallax factor.

TABLE 1
NGC 6853 Log of Observations

Set	MJD	Roll[a] (deg)	V[b]
1.....	49,985.60531	101.91	13.985 ± 0.004
2.....	50,021.33038	103.9	13.979 ± 0.002
3.....	50,172.92498	268.6	14.015 ± 0.003
4.....	50,178.95797	270.4	14.016 ± 0.002
5.....	50,208.6424	286.6	14.012 ± 0.002
6.....	50,233.84447	286.6	14.026 ± 0.002
7.....	50,569.61249	286.0	13.994 ± 0.003
8.....	50,932.79954	286.0	14.007 ± 0.003

[a] Spacecraft roll as defined in the FGS Instrument Handbook (Nelan & Makidon 2002, p. 140).
[b] Average of six to seven observations at each epoch. Errors are internal, not external.

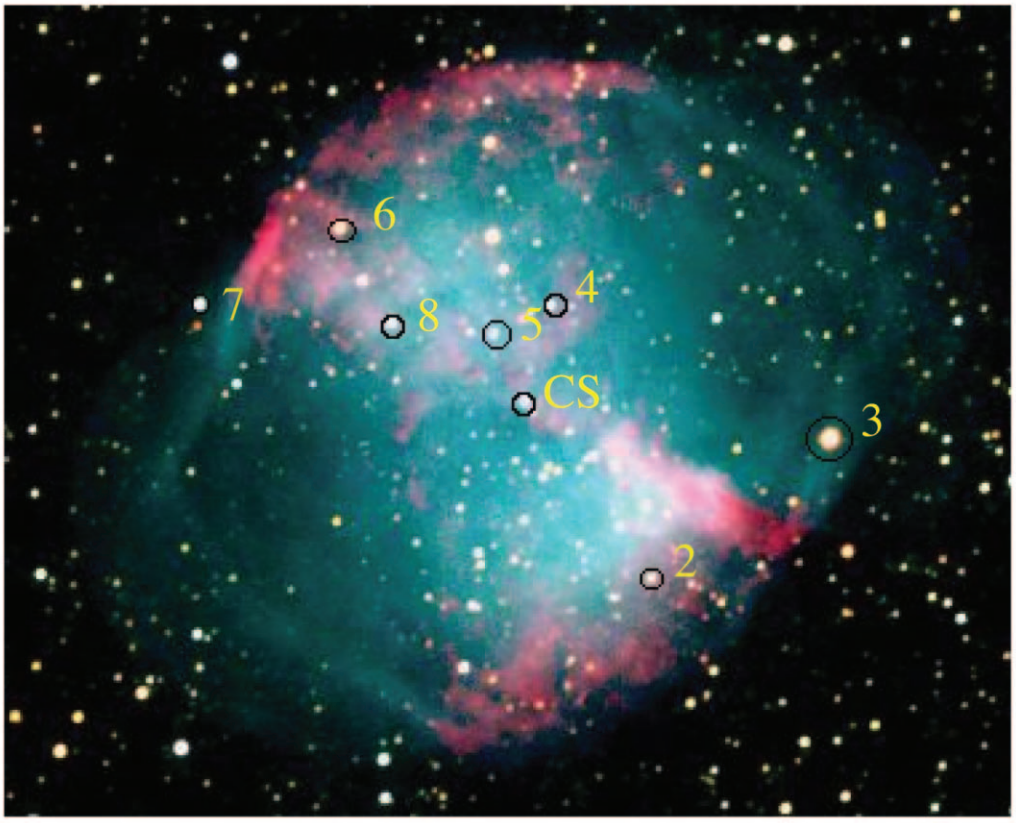

Fig. 1.—NGC 6853 CS and astrometric reference stars. This composite color frame maps Johnson *B*, *V*, and *I* bandpasses as blue, green, and red, respectively. It illustrates potential nebular effects on reference-star photometry and spectroscopy. Exposures were obtained with the McDonald Observatory Prime Focus Camera on the 0.8 m telescope.

TABLE 2
CS and Reference-Star Data

ID	ξ[a]	η[a]	μ_x[b]	μ_y[b]
CS[c]	0.0000 ± 0.0006	0.0000 ± 0.0005	0.0069 ± 0.0005	0.0179 ± 0.0004
Ref-2	−62.9877 ± 0.0007	−90.3490 ± 0.0008	−0.0013 ± 0.0010	0.0052 ± 0.0007
Ref-3	−154.2862 ± 0.0008	−20.5996 ± 0.0009	0.0028 ± 0.0026	−0.0112 ± 0.0020
Ref-4	−13.2770 ± 0.0007	48.4715 ± 0.0007	−0.0066 ± 0.0026	0.0098 ± 0.0021
Ref-5	15.5963 ± 0.0008	34.4350 ± 0.0007	0.0058 ± 0.0031	0.0123 ± 0.0025
Ref-6	93.1016 ± 0.0008	89.0745 ± 0.0008	0.0004 ± 0.0006	0.0020 ± 0.0006
Ref-7	164.5535 ± 0.0010	51.1593 ± 0.0011	0.0026 ± 0.0024	−0.0107 ± 0.0019
Ref-8	67.3571 ± 0.0008	40.5966 ± 0.0008	−0.0064 ± 0.0023	0.0048 ± 0.0019

[a] The variables ξ and η are relative positions in arcseconds.
[b] The variables μ_x and μ_y are relative motions in arcseconds per year.
[c] For this object, R.A. = 19 59 36.2, decl. = 22 43 1.0 (J2000.0), and epoch = MJD 51,486.092. CS position from 2MASS.

3. SPECTROPHOTOMETRIC ABSOLUTE PARALLAXES OF THE ASTROMETRIC REFERENCE STARS

Because the parallax determined for the NGC 6853 CS will be measured with respect to reference-frame stars, which have their own parallaxes, we must either apply a statistically derived correction from relative to absolute parallax (Van Altena, Lee, & Hofleit 1995, hereafter YPC95) or estimate the absolute parallaxes of the reference-frame stars listed in Table 2. In principle, the colors, spectral type, and luminosity class of a star can be used to estimate the absolute magnitude, M_V, and V-band absorption, A_V. The absolute parallax is then simply

$$\pi_{\rm abs} = 10^{-(V-M_V+5-A_V)/5} . \quad (1)$$

The luminosity class is generally more difficult to estimate than the spectral type (temperature class). However, the derived absolute magnitudes are critically dependent on the luminosity class. As a consequence, we obtained additional photometry in an attempt to confirm the luminosity classes. Specifically, we employ the technique used by Majewski et al. (2000) to discriminate between giants and dwarfs for stars later than ~G5, an approach also discussed by Paltoglou & Bell (1994).

3.1. *Photometry*

Our bandpasses for reference-star photometry include *BVRI* (CCD photometry from a 0.4 m telescope at New Mexico State University), *JHK* (from a prerelease of Two Micron All Sky Survey [2MASS]),[13] and Washington/DDO filters *M*, DDO51, and T_2 (obtained at McDonald Observatory with the 0.8 m and Prime Focus Camera). The 2MASS *JHK* bandpasses have been transformed to the Bessell & Brett (1988) system using the transformations provided in Carpenter (2001). The *RI* bandpasses are transformed (Bessell 1979) to the Johnson system from Kron-Cousins measures. Tables 3 and 4 list the visible, infrared, and Washington/DDO photometry for the NGC 6853 reference stars, ref-2 through ref-8.

3.2. *Spectroscopy and Luminosity Class-sensitive Photometry*

The spectra from which we estimated spectral type and luminosity class come from the New Mexico State University Apache Peak Observatory.[14] The dispersion was 1.61 Å pixel^{-1} with wavelength coverage 4101–4905 Å. Classifications used a combination of template matching and line ratios. The brightest targets had about 1500 counts above sky per pixel, or a signal-to-noise ratio of (S/N) ~40, while the faintest targets had about 400 counts per pixel (S/N ~ 20). The spectral types for the higher S/N stars are within ±1 subclass. Classifications for the lower S/N stars are ±2 subclasses. Table 6 lists the spectral types and luminosity classes for our reference stars. The estimated classification uncertainties are used to generate the σ_{M_V} values in that table.

The Washington/DDO photometry can provide a possible confirmation of the estimated luminosity class, depending on the spectral type and luminosity class of the star (later than G5 for dwarfs, later than G0 for giants).

[13] The Two Micron All Sky Survey is a joint project of the University of Massachusetts and the Infrared Processing and Analysis Center.

[14] The Apache Point Observatory 3.5 m telescope is owned and operated by the Astrophysical Research Consortium.

TABLE 3
Visible Photometry

ID	V	$B-V$	$V-R$	$V-I$	$V-K$
CS	13.98 ± 0.03	−0.24 ± 0.04	−0.46 ± 0.04	−0.08 ± 0.04	...
Ref-2	15.41 ± 0.06	2.2 ± 0.2	1.11 ± 0.08	2.19 ± 0.08	3.91 ± 0.06
Ref-3	11.66 ± 0.02	1.87 ± 0.03	1.47 ± 0.03	2.57 ± 0.03	4.52 ± 0.03
Ref-4	14.94 ± 0.03	0.76 ± 0.07	0.59 ± 0.04	1.21 ± 0.04	1.98 ± 0.04
Ref-5	15.45 ± 0.04	0.92 ± 0.07	0.55 ± 0.05	1.18 ± 0.05	2.03 ± 0.05
Ref-6	14.10 ± 0.03	1.95 ± 0.07	1.58 ± 0.04	2.66 ± 0.04	4.63 ± 0.03
Ref-7	13.71 ± 0.03	0.66 ± 0.06	0.49 ± 0.04	1.05 ± 0.04	...
Ref-8	14.69 ± 0.03	1.98 ± 0.07	1.12 ± 0.04	2.13 ± 0.04	4.07 ± 0.04

TABLE 4
ASTROMETRIC REFERENCE-STARS NEAR-IR AND WASHINGTON-DDO PHOTOMETRY

ID	K	$J-H$	$H-K$	M-T_2	M51
Ref-2.....	11.50 ± 0.02	0.74 ± 0.04	0.15 ± 0.04	...	...
Ref-3.....	7.14 ± 0.02	0.89 ± 0.03	0.23 ± 0.03	2.51 ± 0.01	−0.17 ± 0.01
Ref-4.....	12.96 ± 0.03	0.35 ± 0.04	0.13 ± 0.04	1.34 ± 0.10	−0.01 ± 0.14
Ref-5.....	13.42 ± 0.03	0.42 ± 0.04	0.10 ± 0.05	0.56 ± 0.09	−0.02 ± 0.1
Ref-6.....	9.47 ± 0.02	0.81 ± 0.03	0.25 ± 0.03	...	...
Ref-7.....	...	...	...	0.99 ± 0.03	0.10 ± 0.03
Ref-8.....	10.62 ± 0.03	0.80 ± 0.04	0.24 ± 0.04	1.97 ± 0.08	−0.09 ± 0.11

Washington/DDO photometry is less helpful as a discriminator in this case than it has proved for our previous targets (e.g., Benedict et al. 2002b, 2002c; McArthur et al. 2001). As seen in Figure 1, the nebular emission can contaminate the aperture photometry, depending on the filter bandpass. This contamination occurs predominantly in the M filter, because its effective bandpass (4500–5400 Å) includes the strong emission lines at 5007 Å [O III] and 4861 Å Hβ. This results in broadband M-T_2 colors that are slightly bluer than they would be in the absence of the nebula and significantly bluer M-DDO51 indices (M51 in Fig. 2). Additionally, the nebular emission contaminates the sky annulus, which leads to larger measured magnitude errors than would be the case in the absence of the nebula. We list in Table 4 the Washington-DDO photometry. Unfortunately both ref-2 and ref-6 fell on bad columns in the photometer CCD. Figure 3 shows the Washington-DDO photometry along with a dividing line between dwarfs and giants (Paltoglou & Bell 1994). The boundary between giants and dwarfs is actually far " fuzzier " than suggested by the solid line in Figure 3 and complicated by the photometric transition from dwarfs to giants through subgiants. This soft boundary is made readily apparent by Majewski et al. (2000, their Fig. 14). In the absence of contaminating nebular flux, objects just above the heavy line are statistically more likely to be giants than objects just below the line.

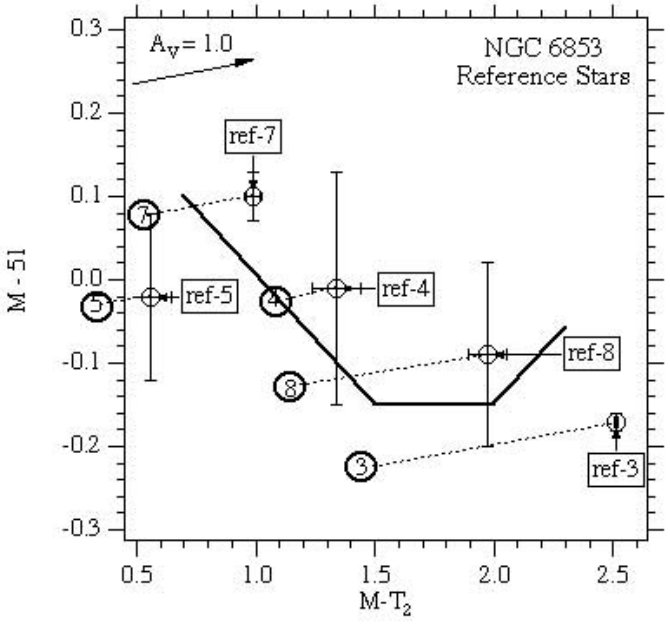

FIG. 2.—M-DDO51 (M51) vs. M-T_2 color-color diagram. The solid line is the division between luminosity class V and luminosity class III stars. Giants are generally above the line, dwarfs below. The reddening vector is for an $A_V = 1.0$. The circled numbers are the reference-star indentifications plotted at the dereddened values, based on the per-star $\langle A_V \rangle$ from Table 5. Nebular emission lines will move objects toward bluer M51 values.

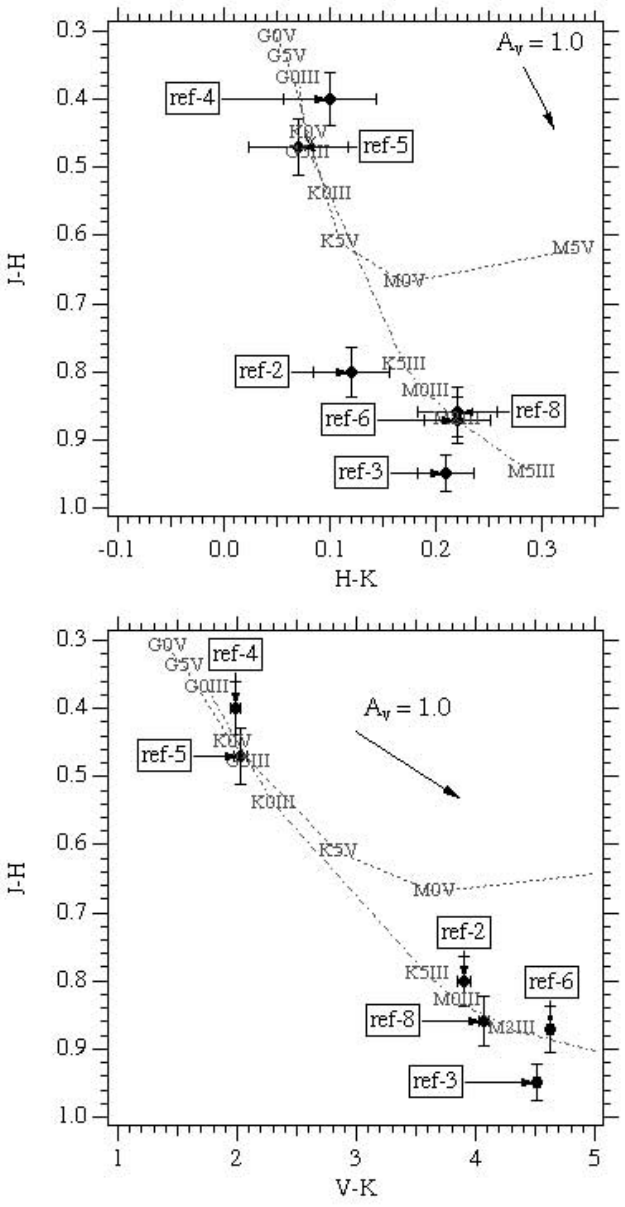

FIG. 3.—$J-H$ vs. $H-K$ and $J-H$ vs. $V-K$ color-color diagrams. The dashed line is the locus of dwarf (luminosity class V) stars of various spectral types; the dot-dashed line is for giants (luminosity class III). The reddening vector indicates $A_V = 1.0$ for the plotted color systems.

TABLE 5
REFERENCE-STAR A_V FROM SPECTROPHOTOMETRY

ID	$A_V(V-I)$	$A_V(V-R)$	$A_V(V-K)$	$A_V(J-K)$	$\langle A_V \rangle$	$\langle A_V \rangle$/100 pc
Ref-2.....	1.64	2.02	1.68	1.68	1.75 ± 0.10	0.05 ± 0.01
Ref-3.....	2.44	2.09	1.59	2.09	2.05 ± 0.20	0.29 ± 0.03
Ref-4.....	0.29	1.13	0.51	0.64	0.64 ± 0.21	0.13 ± 0.04[a]
Ref-5.....	0.04	0.07	0.51	0.81	0.36 ± 0.21	0.04 ± 0.02[a]
Ref-6.....	3.89	3.07	2.43	2.73	3.03 ± 0.36	0.26 ± 0.03
Ref-7.....	0.55	1.27	0.00	0.00	0.91 ± 0.36	0.10 ± 0.04
Ref-8.....	1.37	1.61	1.44	1.97	1.60 ± 0.16	0.05 ± 0.01[a]

[a] Stars used to estimate $\langle A_V \rangle$/100 pc for CS.

After correcting for interstellar extinction, our reference stars lie on the dividing line to the left, where giant/dwarf discrimination is poorest. Nebular emission lines could have depressed ref-3 and ref-8 (giants, as determined from spectroscopy) below the giant-dwarf dividing line.

3.3. *Interstellar Extinction*

To determine interstellar extinction, we first plot these stars on several color-color diagrams. A comparison of the relationships between spectral type and intrinsic color against those we measured provides an estimate of reddening. Figure 3 contains $J-H$ versus $H-K$ and $J-H$ versus $V-K$ color-color diagrams and reddening vectors for $A_V = 1.0$. Also plotted are mappings between spectral type and luminosity class V and III from Bessell & Brett (1988) and Cox (2000; hereafter AQ2000). Figure 3, and similar plots for the other measured colors, along with the estimated spectral types, provides an indication of the reddening for each reference star.

Assuming an $R = 3.1$ galactic reddening law (Savage & Mathis 1979), we derive A_V values by comparing the measured colors (Tables 3 and 4) with intrinsic $V-R$, $V-I$, $J-K$, and $V-K$ colors from Bessell & Brett (1988) and AQ2000. Specifically, we estimate A_V from four different ratios, each derived from the Savage & Mathis (1977) reddening law: $A_V/E(V-R) = 5.1$, $A_V/E(J-K) = 5.8$, $A_V/E(V-K) = 1.1$, and $A_V/E(V-I) = 2.4$. We excluded $A_V/E(B-V)$ due to the higher errors in that color index. The resulting A_V are collected in Table 5. The errors are the standard deviation of the means for each star. We also tabulate A_V per unit 100 pc distance for each star. Colors and spectral types of the NGC 6853 reference stars are consistent with a field-wide average $\langle A_V \rangle = 1.46 \pm 0.35$, far less than the maximum reddening, $A_V < 4.66$ determined by Schlegel, Finkbeiner, & Davis (1998).

3.4. *Adopted Reference-Frame Absolute Parallaxes*

We derive absolute parallaxes with M_V values from AQ2000 and the $\langle A_V \rangle$ derived from the photometry. Our parallax values are listed in Table 6. Individually, no reference-star parallax is better determined than $\sigma_\pi/\pi = 18\%$. The average absolute parallax for the reference frame is $\langle \pi_{\rm abs} \rangle = 1.0$ mas. As a check, we compare this with the correction to absolute parallax discussed and presented in YPC95 (§ 3.2, Fig. 2). Entering YPC95, Fig. 2, with the NGC 6853 galactic latitude, $l = -3\overset{\circ}{.}7$, and average magnitude for the reference frame, $\langle V_{\rm ref} \rangle = 14.3$, we obtain a correction to absolute of 1.1 mas. We will use the 1.0 mas correction derived from spectrophotometry. When such data are available the use of spectrophotometric parallaxes offers a more direct way of determining the reference-star absolute parallaxes.

4. ABSOLUTE PARALLAX OF THE CS OF NGC 6853

4.1. *The Astrometric Model*

With the positions measured by FGS 3, we determine the scale, rotation, and offset "plate constants" relative to an arbitrarily adopted constraint epoch (the so-called master plate) for each observation set (the data acquired at each epoch). The MJD of each observation set is listed in Table 1, along with a measured magnitude transformed from the FGS instrumental system as per Benedict et al. (1998). The NGC 6853 reference frame contains seven stars. We employ the six-parameter model discussed in McArthur et al. (2001) for those observations. In this case, we determined the plate parameters from reference-star data only then apply them as constants to obtain the parallax and proper motion of the CS. For the NGC 6853 field, all the reference stars are redder than the science target. Hence, we apply the corrections for lateral color discussed in Benedict et al. (1999).

As for all our previous astrometric analyses, we employ GaussFit (Jefferys, Fitzpatrick, & McArthur 1987) to minimize χ^2. The solved equations of condition for NGC 6853 are

$$x' = x + {\rm lcx}(B-V)\ , \quad (2)$$

$$y' = y + {\rm lcy}(B-V)\ , \quad (3)$$

$$\xi = Ax' + By' + C + R_x(x'^2 + y'^2) - \mu_x \Delta t - P_\alpha \pi_x\ , \quad (4)$$

$$\eta = -Bx' + Ay' + F + R_y(x'^2 + y'^2) - \mu_y \Delta t - P_\delta \pi_y, \quad (5)$$

where x and y are the measured coordinates from *HST*, lcx

TABLE 6
ASTROMETRIC REFERENCE-STAR SPECTRAL CLASSIFICATIONS AND SPECTROPHOTOMETRIC PARALLAXES

ID	Sp. T.	V	M_V	A_V	$\pi_{\rm abs}$ (mas)
Ref-2.....	K0 III	15.41	0.7 ± 0.4	1.8	0.3 ± 0.1
Ref-3.....	K3 III	11.66	0.3 ± 0.4	2.1	1.4 ± 0.2
Ref-4.....	G3 V	14.94	5.9 ± 0.4	0.6	2.1 ± 0.4
Ref-5.....	G5 V	15.45	5.1 ± 0.4	0.4	1.2 ± 0.5
Ref-6.....	K0 III	14.10	0.7 ± 0.4	3.0	0.8 ± 0.2
Ref-7.....	F4 V	13.71	3.3 ± 0.4	0.9	1.3 ± 0.2
Ref-8.....	K2 III	14.69	0.5 ± 0.4	1.6	0.3 ± 0.1

and lcy are the lateral color corrections from Benedict et al. (1999), and $B-V$ are the $B-V$ colors of each star. A and B are scale and rotation plate constants, C and F are offsets, R_x and R_y are radial terms, μ_x and μ_y are proper motions; Δt is the epoch difference from the mean epoch, P_α and P_δ are parallax factors, and π_x and π_y are the parallaxes in x and y. We obtain the parallax factors from a JPL Earth-orbit predictor (Standish 1990), upgraded to version DE405. We imposed the constraint that the reference-star proper motions are random in direction by forcing their sum in x and y to be zero, $\sum \mu_x = \sum \mu_y = 0$. Orientation to the sky is obtained from ground-based astrometry (USNO-A2.0 Catalog, Monet 1998) with uncertainties in the field orientation $\pm 0\overset{\circ}{.}05$.

4.2. *Assessing Reference-Frame Residuals*

The Optical Field Angle Distortion calibration (McArthur et al. 1997) reduces as-built *HST* and FGS 3 distortions with amplitude $\sim 1''$ to below 2 mas over much of the FGS 3 field of regard. From histograms of the reference-star astrometric residuals (Fig. 4), we conclude that we have obtained satisfactory correction in the region available at all *HST* rolls (an inscribed circle centered on the pickle-shaped FGS field of regard). The resulting reference-frame "catalog" in ξ and η standard coordinates (Table 2) was determined with $\langle \sigma_\xi \rangle = 1.0$ mas and $\langle \sigma_\eta \rangle = 1.0$ mas.

To determine if there might be unmodeled—but possibly correctable—systematic effects at the 1 mas level, we plotted the NGC 6853 reference-frame X and Y residuals against a number of spacecraft, instrumental, and astronomical parameters. These included (X, Y)-position within the pickle, radial distance from the pickle center, reference-star V magnitude and B—V color, and epoch of observation. We saw no obvious trends, other than an expected increase in positional uncertainty with reference-star magnitude.

4.3. *The Absolute Parallax of the NGC 6853 CS*

In a quasi-Bayesian approach, the reference-star spectrophotometric absolute parallaxes were input as observations with associated errors, not as hardwired quantities known to infinite precision. We obtain for the NGC 6853 CS an absolute parallax $\pi_{\rm abs} = 2.10 \pm 0.48$ mas. We note that the formal error on this particular *HST* parallax is larger than we typically achieve with FGS 3. For eight objects in common with *Hippparcos*, we obtain an average parallax precision, $\langle \sigma_\pi \rangle = 0.26$ mas, with no statistically significant scale difference compared with *Hipparcos* (Benedict et al. 2002c, 2002a). We attribute the larger than expected parallax error for the NGC 6853 CS to the less than optimum pattern of maximum positive and negative parallax factors seen in Table 1. However, our result agrees to within the errors with the previous ground-based parallax measurement of the NGC 6853 CS (Harris et al. 1997), $\pi_{\rm abs} = 2.63 \pm 0.43$ mas. Parallaxes from *HST* and *USNO* and relative proper-motion results from *HST* are collected in Table 7. For the remainder of this paper, we adopt as the absolute parallax of the NGC 6853 CS, $\pi_{\rm abs} = 2.40 \pm 0.32$ mas, the weighted average of these two completely independent parallax determinations.

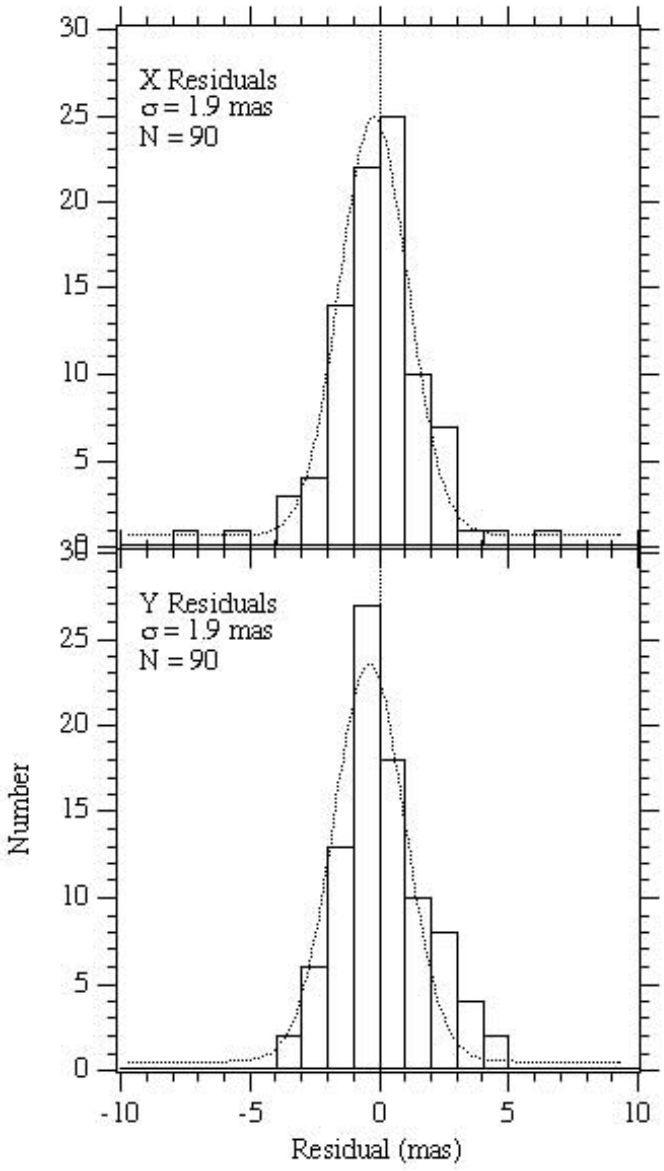

FIG. 4.—Histograms of x and y residuals obtained from modeling the astrometric reference stars with eqs. (4) and (5). Distributions are fitted with Gaussians whose σ values are noted in the plots.

TABLE 7
NGC 6853 PARALLAX AND PROPER MOTION

Parameter	Value
HST study duration (yr)	2.59
Number of observation sets	8
Reference stars $\langle V \rangle$	14.28
Reference stars $\langle B-V \rangle$	1.47
HST absolute parallax (mas)	2.10 ± 0.48
USNO absolute parallax (mas)	2.63 ± 0.43
Weighted average absolute parallax (mass)	2.40 ± 0.32
HST proper motion (mas yr^{-1})	19.2 ± 1.1
Postion angle (deg)	21 ± 1

5. DISCUSSION AND SUMMARY

5.1. *FGS Photometry of the CS*

FGS 3 is a precision photometer, yielding relative photometry with 0.002 mag errors (Benedict et al. 1998). During each of the eight total observation sets, we observed the NGC 6853 CS 6–7 times over approximately 33 minutes. No nonrandom variations were noted within any one data set. The average σ_V for the eight data sets was $\langle\sigma_V\rangle \sim 0.002$ mag. However, statistically significant variations over the 2.6 yr campaign duration are evident in Table 1. Our coverage is too sparse to extract any periodic component to this variation.

5.2. *The Lutz-Kelker-Hanson (LKH) Bias*

When using a trigonometric parallax to estimate the absolute magnitude of a star, a correction should be made for the Lutz-Kelker bias (Lutz & Kelker 1973) as modified by Hanson (1979). Because of the galactic latitude and distance of NGC 6853 and the scale height of the stellar population of which it is a member, we use a uniform space density for determining this LKH bias. The LKH bias is proportional to $(\sigma_\pi/\pi)^2$. Presuming that the CS belongs to the same class of object as RR Lyrae (evolved main-sequence stars), we scale the LKH correction determined for RR Lyrae in Benedict et al. (2002b) and obtain LKH $= -0.15 \pm 0.07$.

5.3. *The Absolute Magnitude of the CS of NGC 6853*

Adopting for the NGC 6853 CS $V = 13.98 \pm 0.03$ and the weighted average absolute parallax, $\pi_{\rm abs} = 2.40 \pm 0.32$ mas from § 4.3, we determine a distance modulus, $(m - M) = 8.10 \pm 0.15$. In Table 5 (§ 3.3), we list a derived per star, per unit 100 pc distance absorption, $\langle A_V\rangle/100$ pc. Given the considerable scatter in that value, we adopt the average of the three stars nearest the central target (see Fig. 1), ref-4, -5, and -8, $\langle A_V\rangle/100$ pc $= 0.07 \pm 0.03$. With this per-unit 100 pc $\langle A_V\rangle$ and the measured distance to the NGC 6853 CS, $d = 417^{+49}_{-65}$ pc, we obtain a total absorption for the CS, $A_V^* = 0.30 \pm 0.06$. As a check, we employ the formulation (Laney & Stobie 1993)

$$R = 3.07 + 0.28(B - V)_0 + 0.04E(B - V) \qquad (6)$$

to obtain for the NGC 6853 CS, $R = 2.99$. From $R = A_V/E(B-V)$, we then obtain $E(B-V) = 0.10$ and a reddening-corrected $B-V = -0.34$, a value one would expect for an object with $T \sim 10^5$ K. For further confirmation of this reddening value, Ciardullo et al. (1999) obtain for NGC 6853 $A_V^* = 0.2 \pm 0.1$ from an $[E(B-V), c]$ relation, assuming a CS temperature of 10^5 K. With $A_V^* = 0.30 \pm 0.06$, we obtain $M_V = 5.43^{+0.28}_{-0.32}$, where we have included the LKH correction and its uncertainty and the 0.06 mag uncertainty in A_V^* in quadrature (for a summary of the astrophysical quantities for NGC 6853, see Table 8).

5.4. *A CS Radius*

To estimate a radius, R_*, for this star, we require a distance, an absolute magnitude, an effective temperature, $T_{\rm eff}$, and a bolometric correction (BC). These quantities then yield a radius via differential comparison with the Sun. Our parallax provides a distance, $d = 417^{+49}_{-65}$ pc, and an absolute magnitude, $M_V = 5.43^{+0.28}_{-0.32}$. Napiwotzki (1999) has estimated $T_{\rm eff} = 108{,}600 \pm 6800$ K from model atmosphere fits to the Balmer Hδ and Hϵ absorption lines.

TABLE 8
NGC 6853 CS Astrophysical Quantities

Parameter	Value	Source
V	13.98 ± 0.03	This paper, Table 3
$B-V$	-0.24 ± 0.04	This paper, Table 3
d (pc)	417^{+49}_{-65}	This paper
A_V^*	0.30 ± 0.06	d and $\langle A_V\rangle/100$ pc for ref-4, 5, 8
$m - M$	8.10 ± 0.15	This paper
LKH Bias	-0.15 ± 0.07	This paper
M_V	$5.43^{+0.28}_{-0.32}$	$m - M$, A_V, LKH bias
$T_{\rm eff}^*$ (K)	$108{,}600 \pm 6800$	Napiwotzki 1999
BC	-7.1 ± 0.20	Flower 1996, Bergeron et al. 1995
$M_{\rm bol}^*$	-1.67 ± 0.37	M_V + BC
R_* ($R_\odot$)	0.055 ± 0.02	This paper
$\mathcal{M}_*$ ($\mathcal{M}_\odot$)	0.56 ± 0.01	Napiwotzki 1999
log g	6.7 ± 0.2, 6.7 ± 0.4	Napiwotzki 1999, this paper

For the BC, we have two sources. Bergeron, Wesemael, & Beauchamp (1995) tabulate BC up to $T_{\rm eff} = 100{,}000$ K from a pure hydrogen, log $g = 8$, DA white dwarf model convolved with a V bandpass. A small extrapolation yields BC $= -7.13$. Flower (1996) provides bolometric corrections for normal stars up to $T_{\rm eff} \sim 54{,}000$ K. From Flower (1996, his Fig. 4), the relationship between log $T_{\rm eff}$ and BC is linear for $T_{\rm eff} > 25{,}000$ K. Hotter stars lie on the Rayleigh-Jeans tail of the blackbody curve, where flux is roughly proportional to $T_{\rm eff}$, not $T_{\rm eff}^4$. A linear extrapolation yields BC $= -7.03$ for the NGC 6853 CS. We adopt BC $= -7.1 \pm 0.2$, where the error is dominated by the uncertainty in $T_{\rm eff}$ and the poorly characterized behavior of the BC at these high temperatures.

We obtain a CS bolometric luminosity $M_{\rm bol} = M_V +$ BC $= -1.67 \pm 0.37$. R_* follows from the expression

$$M_{\rm bol}^\odot - M_{\rm bol}^* = 10\log(T_{\rm eff}^*/T_{\rm eff}^\odot) + 5\log(R_*/R_\odot)\ , \quad (7)$$

where we assume for the Sun $M_{\rm bol}^\odot = +4.75$ and $T_{\rm eff}^\odot = 5800$ K. We find $R_* = 0.05 \pm 0.02$ $R_\odot$. The sources of error for this radius are in the absolute magnitude (i.e., the parallax), the bolometric correction, and the $T_{\rm eff}^*$.

A second way to obtain R_* involves the V-band average flux, H_V, discussed in Bergeron et al. (1995). They list H_V^* as a function of temperature for, again, a pure hydrogen, log $g = 8$, DA model. We obtain H_V^* for $T_{\rm eff} = 108{,}600$ K by a small extrapolation from the highest temperature considered by Bergeron et al. (1995), $T_{\rm eff} = 100{,}000$ K. If we can determine an $H_V^\odot$, we can derive R_* from

$$R_*^2 = (H_V^\odot/H_V^*) \times 10^{-0.4(M_V^* - M_V^\odot)}\ . \qquad (8)$$

In Benedict et al. (2000), where we estimated the radius of Feige 24, the exponent on R_* was inadvertently omitted, but not in the calculation. In that paper, we obtained $H_V^\odot$ by convolving the Bessell (1990) V-band response with the solar spectral distribution listed in Allen (1973). We calculated $H_V^\odot = 6.771 \times 10^5$ ergs cm^{-2} s^{-1} Å^{-1} str^{-1}. We obtain for this CS with $T_{\rm eff} = 108{,}600$ K, $M_V^* = 5.43$ from our parallax, and $M_V^\odot = 4.82$ an $R_* = 0.06 \pm 0.02$ $R_\odot$. As a final check, we calculate R_* from equation (8), but differentially with respect to our Feige 24 M_V (Benedict et al. 2000, Table 5), rather than $M_V^\odot$. This also yields $R_* = 0.06 \pm 0.02$ $R_\odot$. Given that the approach relying directly on the BC and the approach using H_V yield R_* values that agree within

their errors, we adopt $R_* = 0.055 \pm 0.02\ R_\odot$. The error on this radius (2.75 σ) cannot be further reduced by a weighted average of the results from the two approaches, because their errors are highly correlated, both having significant contributions from the uncertainties in $T_{\rm eff}$ and M_V^*.

Comparing with the results presented in Provencal et al. (1998, Fig. 3), and our radius for the hot white dwarf Feige 24, we find the CS of NGC 6853 to have a radius larger than any other white dwarf so far measured. On a log g–log $T_{\rm eff}$ diagram (Napiwotzki 1999, Fig. 2), the evolutionary track of a post-AGB star of a given mass traces a path at first of both increasing log g and log $T_{\rm eff}$. Once the star reaches the WD cooling track, log $T_{\rm eff}$ then decreases, with a smaller rate of change in log g. Having determined both $T_{\rm eff}$ and log g from line profile fitting, Napiwotzki (1999) estimates the mass of the NGC 6853 CS from such a diagram, obtaining $M = 0.56 \pm 0.01\ M_\odot$. A mass and radius uniquely determine a gravity, g,

$$g = MG/R^2\ , \tag{9}$$

where G is the gravitational constant. Our radius, $R_* = 0.055 \pm 0.02\ R_\odot$ and the Napiwotzki (1999) mass yield $\log g = 6.7 \pm 0.4$, in good agreement with the Napiwotzki (1999) line profile fitting value, $\log g = 6.7 \pm 0.2$. Our radius estimate is consistent with a stellar core not yet descended to the white dwarf cooling sequence.

5.5. *Summary*

HST astrometry yields an absolute trigonometric parallax for the NGC 6853 CS, $\pi_{\rm abs} = 2.10 \pm 0.48$ mas. A weighted average with a previous ground-based determination (Harris et al. 1997) provides $\pi_{\rm abs} = 2.40 \pm 0.32$ mas. The higher precision resulting from the average of two independent parallax determinations requires a smaller LKH bias correction, -0.15 ± 0.07 mag. Spectrophotometry of the astrometric reference stars local to NGC 6853 suggest an extinction for the CS, $A_V^* = 0.30 \pm 0.06$. The dominant error terms in the resulting absolute magnitude, $M_V = 5.43^{+0.28}_{-0.32}$, are the parallax and the uncertainty in the amount of extinction for the CS itself. Two methods for estimating the radius of the CS yield $R_* = 0.055 \pm 0.02\ R_\odot$, suggesting a star still above the white dwarf cooling track.

We thank Conard Dahn for his careful and critical refereeing of this paper. Support for this work was provided by NASA through grant NAG 5-1603 from the Space Telescope Science Institute, which is operated by the Association of Universities for Research in Astronomy, Inc., under NASA contract NAS 5-26555. These results are based partially on observations obtained with the Apache Point Observatory 3.5 m telescope, which is owned and operated by the Astrophysical Research Consortium. This publication makes use of data products from the Two Micron All Sky Survey, which is a joint project of the University of Massachusetts and the Infrared Processing and Analysis Center, funded by NASA and the NSF. This research has made use of the SIMBAD database, operated at CDS, Strasbourg, France; the NASA/IPAC Extragalactic Database (NED), which is operated by the Jet Propulsion Laboratory, California Institute of Technology, under contract with NASA; and NASA's Astrophysics Data System Abstract Service.

REFERENCES

Allen, C. W. 1973, Astrophysical Quantities (3d ed.; London: Athlone)
Benedict, G. F., et al. 1999, AJ, 118, 1086
———. 2002a, ApJ, 581, L115
———. 2000, AJ, 119, 2382
———. 2002b, AJ, 123, 473
———. 2002c, AJ, 124, 1695
———. 1998, AJ, 116, 429
Bergeron, P., Wesemael, F., & Beauchamp, A. 1995, PASP, 107, 1047
Bessell, M. S. 1979, PASP, 91, 5
———. 1990, PASP, 102, 1181
Bessell, M. S., & Brett, J. M. 1988, PASP, 100, 1134
Bradley, A., Abramowicz-Reed, L., Story, D., Benedict, G., & Jefferys, W. 1991, PASP, 103, 317
Carpenter, J. M. 2001, AJ, 121, 2851
Ciardullo, R., Bond, H. E., Sipior, M. S., Fullton, L. K., Zhang, C.-Y., & Schaefer, K. G. 1999, AJ, 118, 488
Cox, A. N., ed. 2000, Allen's Astrophysical Quantities (4th ed.; New York: AIP) (AQ2000)
Flower, P. J. 1996, ApJ, 469, 355
Hanson, R. B. 1979, MNRAS, 186, 875
Harris, H. C., Dahn, C. C., Monet, D. G., & Pier, J. R. 1997, in IAU Symp. 180, Planetary Nebulae, ed. H. J. Habing & H. J. G. L. M. Lamers (Dordrecht: Kluwer), 40
Iben, I., & Renzini, A. 1983, ARA&A, 21, 271
Jefferys, W., Fitzpatrick, J., & McArthur, B. 1987, Celest. Mech., 41, 39
Laney, C. D., & Stobie, R. S. 1993, MNRAS, 263, 921
Lutz, T. E., & Kelker, D. H. 1973, PASP, 85, 573
Majewski, S. R., Ostheimer, J. C., Kunkel, W. E., & Patterson, R. J. 2000, AJ, 120, 2550
McArthur, B., Benedict, G. F., Jefferys, W. H., & Nelan, E. 1997, in Proc. 1997 HST Calibration Workshop, ed. S. Casertano, R. Jedrzejewski, T. Keyes, & M. Stevens (Baltimore: STScI)
McArthur, B. E., et al. 2001, ApJ, 560, 907
Monet, D. G. 1998, BAAS, 30, 1427
Napiwotzki, R. 1999, A&A, 350, 101
———. 2001, A&A, 367, 973
Nelan, E., & Makidon, R., eds. 2003, Fine Guidance Sensor Instrument Handbook, Version 11 (Baltimore: STScI)
Paltoglou, G., & Bell, R. A. 1994, MNRAS, 268, 793
Provencal, J. L., Shipman, H. L., Høg, E., & Thejll, P. 1998, ApJ, 494, 759
Savage, B. D., & Mathis, J. S. 1979, ARA&A, 17, 73
Schlegel, D. J., Finkbeiner, D. P., & Davis, M. 1998, ApJ, 500, 525
Standish, E. M., Jr. 1990, A&A, 233, 252
Stanghellini, L., Villaver, E., Manchado, A., & Guerrero, M. A. 2002, ApJ, 576, 285
van Altena, W. F., Lee, J. T., & Hoffleit, E. D. 1995, Yale Parallax Catalog (4th ed.; New Haven: Yale Univ. Obs.) (YPC95)